Dielectric Relaxation in Transfer Media for Electrophotography

Inan Chen and Ming-Kai Tse
Quality Engineering Associates, Inc.
755 Middlesex Turnpike, Unit 3, Billerica MA 01821
Tel: 978-528-2034 · Fax: 978-528-2033
e-mail: info@qea.com
URL: www.qea.com

Paper presented at Japan Hardcopy 2000
The Imaging Society of Japan
July 2000, Tokyo, Japan

Japan Hardcopy 2000, Tokyo (Jun.12, 2000)

Dielectric Relaxation in Transfer Media for Electrophotography

Inan Chen* and Ming-Kai Tse**

*Consulting Scientist, **QEA, Inc. Burlington, Massachusetts, USA

Abstract: In electrostatic transfer of developed toners to receiving media, efficient dielectric relaxation in the media enables efficient transfer at moderate bias voltages. Using the first principle treatment of charge transport in semi-insulators, we show that dielectric relaxation in transfer media is determined not simply by resistivity and permittivity but more precisely by charge density, mobility and injection properties at the contacts. A novel experimental technique for characterizing dielectric relaxation in transfer media has been devised to permit better prediction of performance in electrostatic transfer. Results from representative media samples are presented and discussed.

Introduction

In electrostatic (ES) transfer of developed toners to receiving media such as paper or intermediate belts (hereafter "receiver"), a bias voltage is applied across a multi-layer consisting of the receiver, the toner layer, the photoreceptor, and a small air gap (Fig. 1). Because the receiver is so thick relative to the other layers, successful transfer depends on dielectric relaxation in the receiver causing a large fraction of the applied voltage to shift to the toner layer. Traditionally, dielectric relaxation is described by an equivalent circuit model, representing the layers by their resistances and capacitances.[1] However, experimental data on semi-insulating materials such as those used for transfer media have shown that dielectric relaxation does not always follow the exponential time dependence predicted by the equivalent circuit model.[2,3] A mathematical model has been developed for treatment of charge transport in semi-insulators[3,4] taking into consideration space-charge effects and features such as non-Ohmic charge injection, charge trapping, and field dependent mobility. In this paper, we apply this model to dielectric relaxation in ES transfer.[5] The two components of conductivity – charge density and mobility – are shown to play independent roles. Charge density determines the extent of transfer, while charge mobility determines the time required for achieving transfer. Thus, in high-speed printers with limited process time, it becomes important to specify the minimum requirements for both charge density and mobility, not just their product, conductivity.

For the purpose of achieving better prediction of performance in ES transfer, a novel experimental technique known as electrostatic charge decay (ECD) is applied to transfer media.[6-7] Results from representative media samples are presented to demonstrate the effectiveness of the technique.

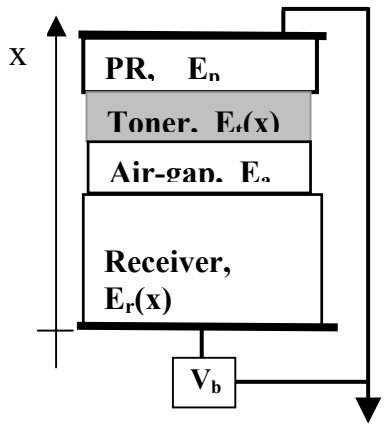

Figure 1. One-dimensional schematic of transfer nip

Space-Charge Model of Electrostatic Transfer

A one-dimensional schematic of the multi-layer configuration at the transfer nip is shown in Fig. 1. The photoreceptor (PR) and the air-gap are assumed to be space-charge free, and hence the fields E_p and E_a are spatially uniform. The toner layer is assumed to have a constant volume charge density q_t, and thus the field $E_t(x)$ is a linear function of the product $q_t x$. The conductivity of the receiver is $\sigma = (\mu_p + \mu_n)q_i$, where μ denotes the drift mobilities of holes and electrons, and q_i is the intrinsic charge density.

When a bias voltage V_b is applied across the multi-layer, the current in the receiver (attributable to the intrinsic charge and the injected charge from the bias electrode) causes the voltage across the receiver to decay with time, and the voltages across the other layers to increase with time. The time and spatial

** 99 South Bedford Street #4, Burlington MA 01803 USA

variations of charge densities are governed by the continuity equations. The field in the receiver $E_r(x)$ can be calculated from the space-charge densities according to Poisson's equation. The fields on both sides of an interface are related by Gauss' theorem to the interface charge density. Due to the non-homogeneity of receivers, the drift mobility is likely to be field dependent. For lack of better knowledge, it is represented by the following power-law,

$$\mu(E) = \mu_o(E/E_o)^k \quad (1)$$

where μ_o denotes the mobility at a nominal field E_o and k is the power. The mobility may not be the same for holes and electrons. The charge injection into the receiver from the bias electrode is specified assuming the injection current $J_i(0, t)$ to be proportional to the field at the boundary,

$$J_i(0, t) = sE_r(0, t) \quad (2)$$

where the proportionality constant s has the dimension of conductivity. Starting with the initial conditions that the receiver is charge neutral, that there is no charge accumulated at the receiver/air-gap interface, and that the layer voltages are divided capacitively at t = 0, the fields and voltages in each layer can be calculated as functions of time by a numerical procedure.[3-5]

Layer Voltages

Figure 2 shows the time evolution of the voltage across the receiver calculated with the space-charge model using a set of typical parameter values for "discharge area development." The voltage is normalized to the initial voltage across the receiver, $V_r(0)$. The time is in units of a nominal transit time defined by

$$t_T \equiv L_r^2/\mu_o V_b \quad (3)$$

where L_r is the receiver thickness. In the case of field dependent mobility (dashed curves), t_T is defined with the mobility μ_o at a nominal field $E_o = V_b/L_r$. It can be seen from the semi-log plot that the decay of receiver voltages does not follow the simple exponential form. A comparison of the solid and dashed curves indicates that this feature is enhanced by field dependent mobility. Calculations are carried out to confirm that this feature is qualitatively independent of the choice of parameter values within the range of practical interest.

Transfer Efficiency

The field in the toner layer can be written as

$$E_t(x) = E_{t0} + q_t(x - x_{t0})/\varepsilon_t \quad (4)$$

where E_{t0} is the field at the toner-air interface x_{t0}, and ε_t is the permittivity of the toner layer. For negative toners to be transferred, this field must be positive. Thus, the amount of toner transferred can be determined (neglecting the adhesive forces) by the position x where the field $E_t(x)$ changes sign. The transfer efficiency is given by the ratio of such $(x - x_{t0})$ to the toner layer thickness L_t.

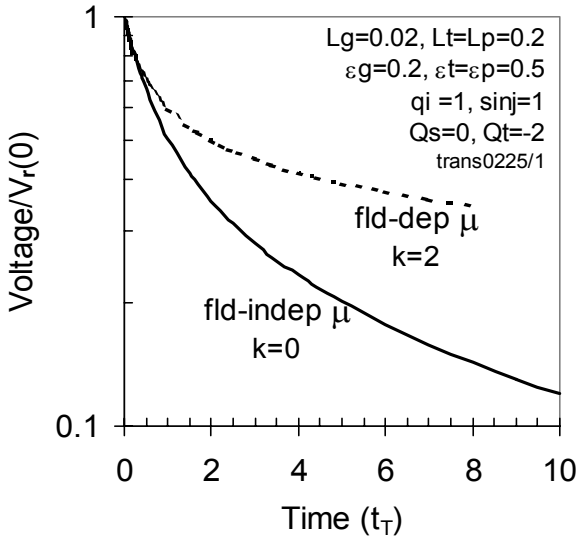

Figure 2. Examples of calculated receiver layer voltage vs. time, for field independent mobility (solid curve) and field dependent mobility (dashed curve).

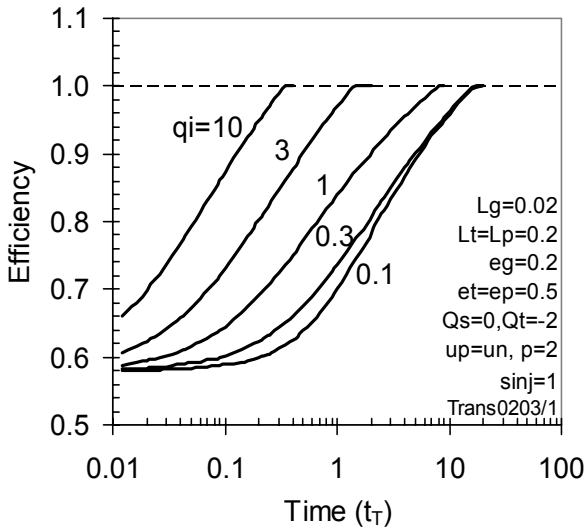

Figure 3. Transfer efficiency vs. time for various intrinsic charge densities q_i, calculated for field-dependent mobility (k=2).

Calculated examples of transfer efficiency as a function of time are shown in Fig.3 for samples with various intrinsic charge densities q_i, assuming a good injection from the electrode. q_i is given in units of q_o defined by

$$q_o \equiv \varepsilon_r V_b/L_r^2 = C_r V_b/L_r \quad (5)$$

where ε_r is the permittivity of the receiver, and C_r is the receiver layer capacitance.

Full transfer, i.e. transfer efficiency reaching unity, is important for preventing color shifts. It can be seen that the time required to reach full transfer t_F increases as q_i decreases.

Using data similar to those in the figure above, Fig. 4 plots time t_F versus intrinsic charge density q_i for different injection conditions specified by the parameter s, defined in Eq. (2). t_F is expressed as a multiple of t_T ($t_F = m\ t_T$), q_i as a multiple of q_o, ($q_i = nq_o$), and s in units of $s_o = \varepsilon_r\mu_o V_b/L_r^2$. The mobility is assumed to be quadratically field dependent, i.e. k = 2 in Eq.(1). Quantitatively different but qualitatively similar results are obtained with different forms of field dependence.

With larger values of q_i ($n \approx 10$), t_F is insensitive to the injection condition (s), because the intrinsic charge is sufficient for completing dielectric relaxation in the receiver. For smaller q_i ($n < \approx 1$), the dielectric relaxation depends critically on the injected charge, and hence t_F varies significantly with the s values but is insensitive to q_i.

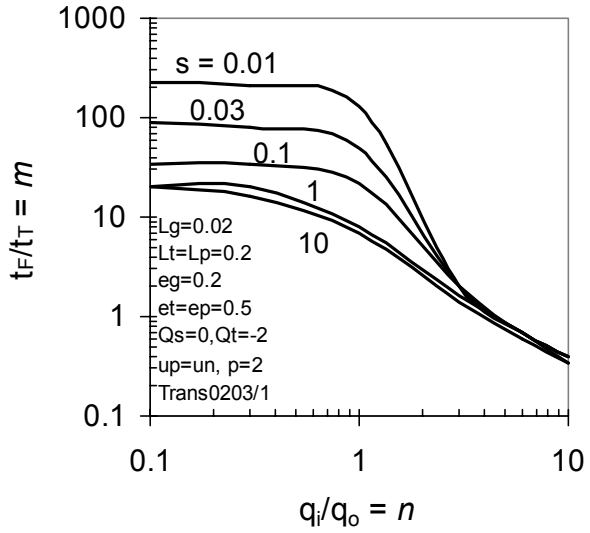

Figure 4. Time to full transfer (in units of t_T), vs. intrinsic charge density (in units of q_o), for various injection conditions, specified by parameter s defined in Eq.(2).

In principle, the process time t_{proc} must be long enough for full transfer. Using the definition of t_T from Eq.(3), this can be written as,

$$t_{proc} \geq t_F = mt_T = m(L_r^2/\mu_o V_b) \qquad (6)$$

Thus, for full transfer to occur within the process time, the mobility μ_o must be larger than a value related to the layer thickness L_r, the bias V_b, the process time t_{proc} and the factor m as

$$\mu_o \geq m(L_r^2/t_{proc}V_b) \approx m(10^{-6}\ \mathrm{cm^2/Vsec}) \qquad (7)$$

The numerical value in parentheses is calculated for a process time of 0.1 sec, a typical thickness $L_r \approx 10^{-2}$ cm and bias $V_b \approx 10^3$V.

Using Eqs.(5) and (7), the conductivity required for full transfer within the process time can be expressed in terms of m and n as

$$\sigma \approx 2\mu_o q_i \geq mn(2\varepsilon_r/t_{proc}) \approx mn(10^{-11}\ \mathrm{S/cm}) \qquad (8)$$

where $\varepsilon_r = 5\mathrm{x}10^{-13}$ F/cm and $t_{proc} = 0.1$ sec are used to obtain the numerical value in parentheses. A plot of the product mn vs. n, from the data in Fig. 4 is shown in Fig. 5. The product mn is seen to have a value (≈ 4) independent of q_i and s only for large $q_i \geq 3q_o$. This means that the required conductivity cannot be specified without knowing q_i and s. For example, with $q_i \approx q_o$ ($n \approx 1$) the required conductivity increases by an order of magnitude or more as the injection level s decreases. In other words, the conductivity is not a single figure of merit for full transfer. Instead, the transfer efficiency is determined collectively by the three ingredients of dielectric relaxation, namely, intrinsic charge density q_i, mobility μ_o and injection s.

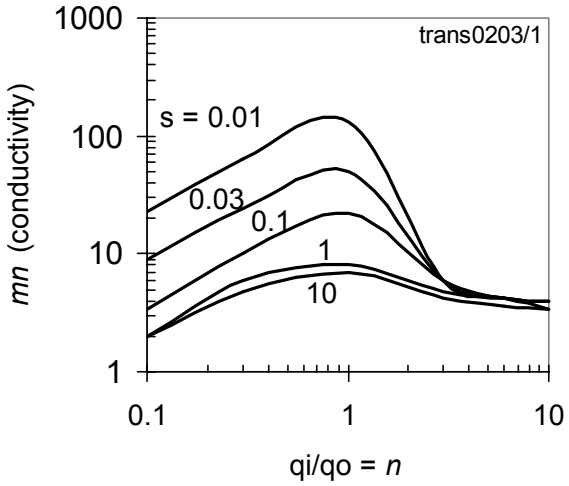

Figure 5. Conductivity required for full transfer, represented by mn, as a function of q_i (or n), for various injection conditions (s).

Experiments

Based on the above principle, the "electrostatic charge decay" (ECD) technique, previously introduced for characterizing photoreceptors and charge roller coatings,[6,7] is applied as a novel technique for monitoring dielectric relaxation of media. When applied to transfer media, the sample on a grounded substrate is corona-charged for a finite time. The subsequent decay of the surface voltage, due to dielectric relaxation induced by the intrinsic charge in the sample and the charge injected from the substrate, is monitored with an electrostatic voltmeter.

Two examples of data from electrophotographic paper samples are shown in Fig. 6. Because of the spatial separation between the corona charger and the voltage probe, a short delay occurs between the end of charging and the beginning of voltage measurement. The decay is obviously non-exponential. The difference in voltages at the first data points indicates that dielectric relaxation during the charging time is more efficient in sample PP-1 than in PP-2. This trend continues in the decay after charging.

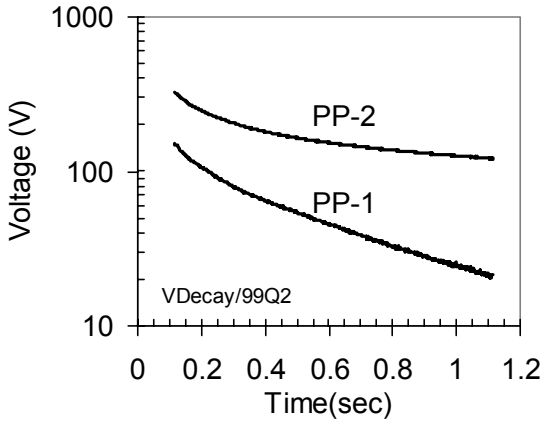

Figure 6. Electrostatic charge decay (ECD) curves of two paper samples.

Similar ECD data from a set of intermediate transfer belts are shown in Fig. 7. The belts Gn and Gu, which perform well in toner transfer, show more efficient decay (and dielectric relaxation) than do Bn and Bu, which show poorer transfer performance. The voltages at the first data points are very close for the new (n) and used (u) samples in both the good and bad pairs, but the long time decays after charging are quite different. This can be attributed to the fact that the initial decay during charging is driven mainly by the intrinsic charge, which is unlikely to be affected by usage, while the decay after charging depends more on injected charge, which can be significantly affected by surface deterioration from usage.

The detailed procedure for a more quantitative determination of the pertinent electrical parameters mentioned above, intrinsic charge density, mobility and injection level, will be presented in later publications.

Summary and Conclusions

A first principle treatment of charge transport has been applied to dielectric relaxation in receiving media during ES transfer. Based on the conditions for full transfer, the minimum required charge mobility can be shown to increase as the process speed increases, as the intrinsic charge density decreases, and/or as the charge injection from the contact decreases.

Consequently, the traditional approach of predicting the performance of a receiver by its conductivity, i.e. the product of intrinsic charge density and mobility, is shown to be insufficient and sometimes meaningless.

Thus, characterization of receiver performance in ES transfer must ideally be carried out under conditions closely simulating the charge supply and transport in the actual printing application. The effectiveness of the electrostatic charge decay (ECD) technique for this purpose has been demonstrated.

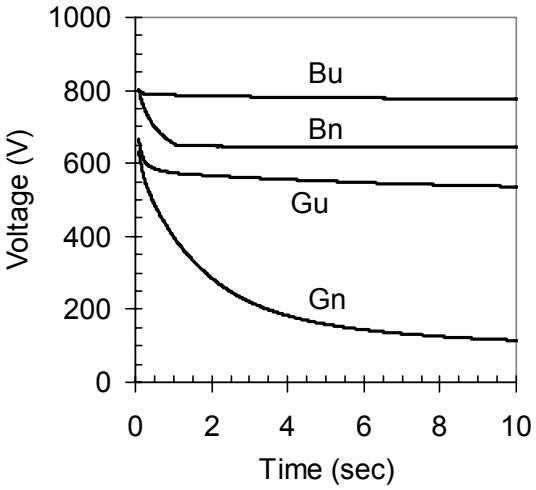

Figure 7. ECD curves of four intermediate transfer belts. Gn and Gu are new and used belts, respectively, that perform well. Bn and Bu are new and used belts that perform poorly.

References

1. M. C. Zaretsky, *J. Imag. Sci. & Tech.* **37**, 187 (1993); J. W. May and T. N. Tomb, Proc. of NIP13, p.71 (1997); T. N. Tomb, Proc. of NIP14, p.440 (1998)
2. M.-K. Tse and I. Chen, Proc. of NIP14, p. 481 (1998)
3. I. Chen and M.-K. Tse, Proc. of NIP15, p.486 (1999); also Japan Hardcopy 99, p.137. (1999)
4. I. Chen, J. Mort, M. A. Machonkin, J. R. Larson, and F. Bonsignore, *J. Appl. Phys*. **80**, 6796 (1996)
5. I. Chen and M.-K.Tse, Proc. of NIP15, p.155 (1999)
6. M. K. Tse, Proc. of NIP 10, p.295, (1994); M. K. Tse and A. H. Klein, Proc. of PPIC/JHC, (1998)
7. M. K. Tse, D. J. Forest, and F. Y. Wong, Proc. of NIP11, p.383 (1995); Proc. of NIP15, p.159 (1999).